Proceedings of the Canadian Society for Mechanical Engineering International Congress 2021
CSME Congress 2021
June 27-30, 2021, Charlottetown, PE, Canada

Artificial Neural Network Based Crystal Plasticity Framework to Simulate Flow Behavior In Aluminum Alloys

Usman Ali[1,2]
[1]Department of Mechanical Engineering, King Fahd University of Petroleum & Minerals, Dhahran, 31261, Saudi Arabia
[2]Interdisciplinary Research Center on Advanced Materials, King Fahd University of Petroleum & Minerals, Dhahran, 31261, Saudi Arabia

Abstract — Machine learning techniques are used to understand and predict data trends. The flexibility of machine learning approaches such as artificial neural networks (ANN) has seen these approaches being used in various applications. As experimental methods are costly and time-consuming, numerical simulations are often used for their predictive capabilities. In this work, ANN framework is proposed to predict the stress-strain and texture evolution response under simple shear. Stress-strain response from individual crystals were trained and validated with the ANN model to predict the polycrystalline response. Results from the ANN model were compared to experimental simple shear stress-strain results and show good agreement.

Keywords; crystal plasticity; artificial neural networks;

I. INTRODUCTION

Numerical simulations provide a commercially viable method to predict material response for engineering design. Experimental techniques are the default method to measure the material response but due to high experimental cost, designers prefer numerical models to simulate material response under complex loading conditions. However, as the complexity of numerical models increase, these models require costly setups and material models which are not available in commercial softwares.

Machine learning approaches such as artificial neural networks (ANN) provide a flexible alternative to numerical models. ANN models simulate a neuron in the brain that learns with training through available data. In addition, the flexibility of ANN models does not require implementation of complex or unknown physical relationships for predicting the material response [1], [2]. Results in literature show that ANN models show excellent predictive capabilities when compared to experimental results. Bhadeshia [3] has discussed some of the applications of ANN models in materials science. In addition, several researchers have used ANN for various applications in materials science to predict the material response. For example, ANN models have been used to predict the flow behavior for various steel and aluminum alloys at room and elevated temperatures [4]–[7]. ANN models have also been used to predict material damage under cyclic loading [8]–[11]. Recently, ANN models have also been used to predict local strain distributions [12] and forming limit diagrams (FLD's) [13] for various metallic alloys. Even though ANN models have been used for various applications, literature lacks works in predicting texture dependent stress-strain response. In addition to the predictive capabilities, ANN models offer a computationally efficient solution. Compared to numerical models, ANN models provide huge time savings over commonly used simulation techniques.

It is well known that texture and more specifically, microstructure plays an important role in material stress-strain response. Therefore, prediction of flow behavior should be dependent on the material microstructure. Researchers have used ANN models to predict microstructure related properties of materials such as grain size [14], rolling textures [15], steel phases [16] etc. In addition, ANN models have also been used to find optimum microstructures for desirable properties [17]. Results from these works show the flexibility of ANN models to adapt to predict complex physical systems and provide accurate predictions for various materials. However, literature lacks prediction of texture dependent flow behavior using ANN models.

In this work, an ANN framework is used to predict the stress-strain response of AA6063-T6 under simple shear. The stress-response is dependent on the initial texture of the material. The ANN model is created based on commonly found single crystal textures to predict the polycrystalline response. The single crystal data set for the ANN models is obtained from a Taylor based in-house crystal plasticity model [18], [19]. ANN predictions for the polycrystalline response are compared to experimental stress-strain results and show good agreement. The computational efficiency of ANN models is also compared to crystal plasticity simulations. Results shown in the work highlight the importance of ANN models for accurate and timely material behavior predictions.

II. Material Characterization

Commercially available aluminum alloy (AA6063-T6) used in this study had a nominal thickness of 1.8 mm. Simple shear tests were performed using a modified ASTM B831-14 sample geometry [20], [21]. The tests were performed using an MTS Landmark 370 Servo-hydraulic tensile machine with a load cell of 100 KN at 1.0 mm/min. Strain evolution during the test was captured using a digital image correlation (DIC) system (ARAMIS™) at 1 fps. The shear angles θ were averaged to find the shear strain's γ using $\gamma = tan\theta$. To capture the initial microstructure, Electron Backscatter Diffraction (EBSD) was performed using a field-emission Nova NanoSEM™ equipped with a TSL EBSD camera with a step size of 0.5 µm [19].

The stress-strain and microstructure of AA6063-T6 is shown in Figure 1. The stress-strain response shows a typical simple shear behavior observed in several aluminum alloys. The final inverse pole figure (IPF) map is also shown in Figure 1 with an average grain size of 65 µm. The <111> pole figure is shown in Figure 1 and shows a predominantly Cube and Goss texture. As Cube and Goss are the predominant textures, these textures will be used to train the proposed ANN model.

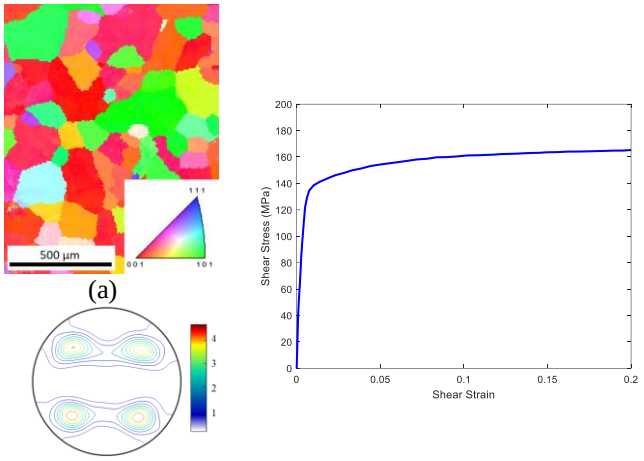

Figure 1: (a) Inverse pole figure (IPF) map for as-received material (b) Corresponding <111> pole figure (c) Simple shear stress-strain curve

III. Crystal Plasticity Framework

Phenomenological models are the most commonly used material models for capturing the material stress-strain behavior [22], [23]. However, they cannot capture the microstructure evolution during deformation. In addition, incorporating microstructure dependent flow behavior is challenging. Crystal plasticity formulations offer a viable solution as they use crystallographic slip to predict the material behavior and therefore can account for the microstructure. These formulations have been used by several researchers to predict the flow behavior under various loading conditions [24]–[26].

The Taylor based rate-dependent crystal plasticity formulation used in this work accounts for the plastic deformation on 12 <110> and <111> slip systems [27] and is given by:

$$\hat{\boldsymbol{\sigma}} = \boldsymbol{LD} - \dot{\boldsymbol{\sigma}}^{\boldsymbol{0}} - \boldsymbol{\sigma}\, \boldsymbol{tr}\boldsymbol{D} \tag{1}$$

where $\hat{\sigma}$ is the Jaumann rate of Cauchy stress, D is the strain-rate tensor, L is the elastic stress tensor and $\dot{\sigma}^0$ is the viscoplastic type stress state.

Slip rates for each slip system α are given as:

$$\dot{\gamma}_\alpha = \dot{\gamma}_0 sgn\ \tau_\alpha \left|\frac{\tau_\alpha}{g_\alpha}\right|^{1/m} \tag{2}$$

where $\dot{\gamma}_0$ is the reference shear rate, τ_α is the resolved shear stress, m is the strain-rate sensitivity index and g_α is the slip system hardness.

Similarly, work hardening is given as:

$$\dot{g}_\alpha = \sum_\beta h_{\alpha\beta} \left|\dot{\gamma}_\beta\right| \tag{3}$$

where $h_{\alpha\beta}$ are the hardening moduli such as:

$$h_{\alpha\beta} = q_{\alpha\beta} h_\beta \text{ (no sum on } \beta) \tag{4}$$

where $q_{\alpha\beta}$ defines the latent hardening behavior of the crystal and h_β is the single crystal hardening [28] and is given as:

$$h_\beta = h_s + (h_0 - h_s) sech^2 \left[\left(\frac{h_0 - h_s}{\tau_s - \tau_0}\right)\gamma_\alpha\right] \tag{5}$$

where h_0 and h_s are the hardening rates and τ_s is the saturation shear stress, if $h_s = 0$.

IV. Artificial Neural Network Model

In this work, an ANN model is used to predict the stress-strain response from single crystals. Other machine learning models such as ReLu could also be used but ANN was used due to its flexibility and success with various engineering related problems. The starting microstructure and strain-rate in the proposed ANN model are used as inputs to the ANN framework while the complete stress-strain response from crystal plasticity single crystal numerical simulations are used as outputs from the ANN framework.

A typical ANN model consists of Input and Output layers with single or multiple neurons in each layer as shown in Figure 2. A feed forward back propagation ANN is used in this work to provide a flexible model [30]. In this model, the outputs and inputs are connected by a function $\boldsymbol{f}$ which is found by minimizing the cost function C. The cost function is taken as an average of the individual cost functions C_x and is given as:

$$C = \frac{1}{n}\sum_x C_x \tag{6}$$

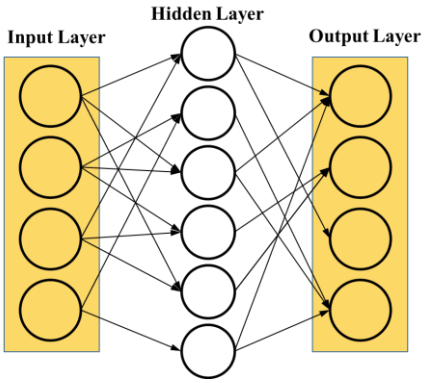

Figure 2: Artificial neural network visualization

Similarly, the neurons which are part of a particular layer are given as:

$$y = \varphi\left(\sum_{i=1}^{d} w_i x_i + b_i\right) \tag{7}$$

where w_i and b_i are the weights and bias of the i-th input in the ANN model, d is the number of inputs in the input vector, x, and φ is the activation function. The interconnected layers dictate that the output from one layer acts as an input to the next layer. For example, Figure 2 shows an ANN model with 4 outputs and inputs with 6 neurons. The inputs and outputs are implemented as:

$$\boldsymbol{a_j} = \boldsymbol{\varphi}\left(\boldsymbol{w_j} \cdot \boldsymbol{a_{j-1}} + \boldsymbol{b_j}\right) \text{ for } 1 \le j \le L \text{ and } a_0 = x \tag{8}$$

$$\mathbf{y} = \varphi(\boldsymbol{V} \cdot \boldsymbol{a_L}) \tag{9}$$

where L is the number of layers, $\boldsymbol{a_L}$ are the activation vectors for each neuron in layer L and $\boldsymbol{V}$ are the model parameters.

The weight matrices $\boldsymbol{w_1}, \ldots, \boldsymbol{w_L}$, the vectors of biases $\boldsymbol{b_1}, \ldots, \boldsymbol{b_L}$ and model parameters $\boldsymbol{V}$ are learned from the input data set $\boldsymbol{x}$ for the optimal function $\boldsymbol{f}$. A backpropagation algorithm is used to find the cost function gradients as it is one of the most commonly used approach [32]. Efficiency of the backpropagation algorithm is measured using an average square error between the outputs $\boldsymbol{f}(\boldsymbol{x})$ and target values $\boldsymbol{y}$ [33].

The activation function for each neuron can be specified by various functions [34], [35]. However, the hyperbolic tangent sigmoid function is most commonly used and is given as:

$$\varphi(n) = \frac{2}{(1 + e^{-2n})} - 1 \tag{10}$$

Finally, the ANN model is broken down into training (70%), validation (70%) and test (70%) sets. The training and validation datasets are used to make the ANN model while the test set is new data that is used to validate and measure the effectiveness of the model. In this work, the input strain ε and initial microstructure ϕ_1, ϕ, ϕ_2 is taken as the input to the ANN model while the corresponding stress σ is taken as the model output for single crystal. The polycrystalline stress-strain behavior of the model is predicted based on the single crystal results.

V. Results and Discussion

A. *Crystal plasticity results*

Rate-dependent crystal plasticity model described earlier was used to model the texture dependent stress-strain behavior of AA6063-T6 under simple shear. The simulation parameters used for the crystal plasticity simulations is shown in Table 1.

Table 1: Crystal plasticity simulation parameters

m	q	h_0/τ_0	h_s/τ_0	τ_s/τ_0	τ_0
0.02	1.0	2.08	0.14	1.18	61.0

The corresponding texture results are shown in Figure 3. It should be noted that as Cube (0, 0, 0) and Goss (0, 45, 0) constitute the majority of the texture components in AA6063-T6, only these texture components were modeled using the crystal plasticity simulations.

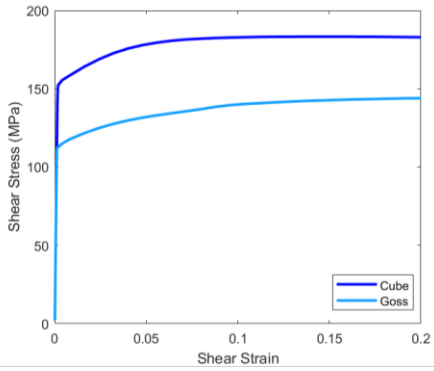

Figure 3: Single crystal Goss and Cube stress-strain results under simple shear.

B. *Artificial neural network results*

The crystal plasticity single crystal stress-strain results were used as inputs to the ANN model. Both texture components were trained together so incorporate the interdependency between texture components. The corresponding results from the crystal plasticity (XP) simulations and artificial neural network (ANN) results are shown in Figure 4. Results show an excellent match with both the Cube and Goss component stress-strain results. The stress-strain results are able to capture both the elastic and plastic response of the single crystal results. The average MSE error was also calculated for the Cube and Goss ANN predictions (Table 2). Results show an MSE error in the order of 10^{-5} thus showing the high level of accuracy achievable by ANN models.

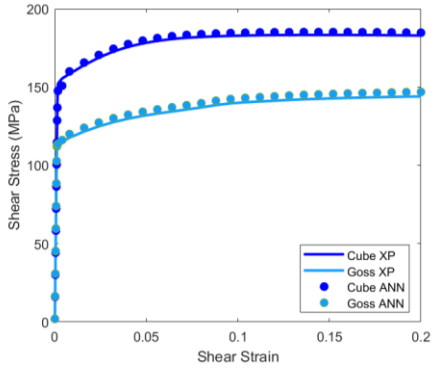

Figure 4: Crystal plasticity (XP) and artificial neural network (ANN) Single crystal Goss and Cube stress-strain results under simple shear.

The validation of the ANN model with single crystal results enables the use of the ANN model to be used for polycrystalline predictions. Therefore, the ANN model was used to predict the polycrystalline AA6063-T6 behavior using the ANN predictions. It should be noted that as the ANN model was not trained on all possible texture components, a higher error should be expected. Figure 5 shows the comparison between experimental (EXP) and artificial neural network (ANN) predictions on the polycrystalline stress-strain response of AA6063-T6 under simple shear. Comparison between the experimental and ANN predictions also serves as a validation for this work. The MSE for the polycrystalline ANN predictions was calculated as 1.74 x 10^{-3} (Table 2). ANN predictions show an excellent agreement with experimental results with high accuracy. A little discrepancy is noted near the yield point and at 20% shear strain. In addition, compared to single crystal results, polycrystalline show a relatively high error. These differences are due to the limited texture components used in training the ANN model.

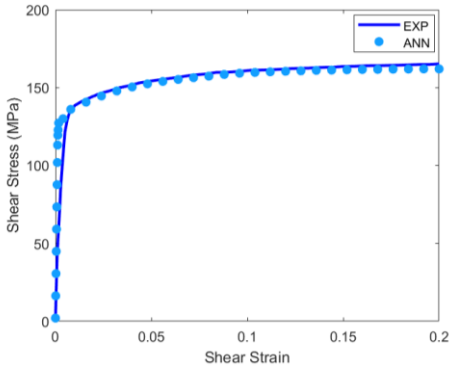

Figure 5: Comparison between experimental (EXP) and artificial neural network (ANN) polycrystalline simple shear response.

Table 2: Mean squared errors from ANN model results

	Error
Cube	4.0 x 10^{-5}
Goss	3.95 x 10^{-5}
Polycrystal	1.74 x 10^{-3}

VI. CONCLUSIONS

In this work, an artificial neural network (ANN) framework was proposed to simulate texture dependent stress-strain behavior. The proposed methodology was applied on AA6063-T6 under simple shear. Crystal plasticity single crystal simulations were conducted on the major texture components found in the as-received material. The output from crystal plasticity simulations was used as input to the ANN model. Single crystal ANN predictions showed excellent results with a MSE of 10^{-5}. Validated ANN model was then used to predict the polycrystalline AA6063-T6 response under simple shear. The ANN model showed excellent agreement with experimental results. The framework proposed in this work shows the strength and flexibility of ANN models for fast and accurate prediction of material behaviors under various initial and loading conditions.

ACKNOWLEDGMENTS

The authors would like to acknowledge the help and support of Mechanical Engineering Department at King Fahd University of Petroleum & Minerals (KFUPM). In addition, the authors would like to acknowledge Dr Waqas Muhammad for help with the experimental work.

REFERENCES

[1] A. Jenab, A. Karimi Taheri, and K. Jenab, "The use of ANN to predict the hot deformation behavior of AA7075 at low strain rates," *J. Mater. Eng. Perform.*, vol. 22, no. 3, pp. 903–910, 2013, doi: 10.1007/s11665-012-0332-y.

[2] U. Ali *et al.*, "Experimental investigation and through process crystal plasticity-static recrystallization modeling of temperature and strain rate effects during hot compression of AA6063," *Mater. Sci. Eng. A*, vol. 700, pp. 374–386, Jul. 2017, doi: 10.1016/j.msea.2017.06.030.

[3] H. K. D. H. Bhadeshia, "Neural Networks in Materials Science.," *ISIJ Int.*, vol. 39, no. 10, pp. 966–979, 1999, doi: 10.2355/isijinternational.39.966.

[4] Y. C. Lin, J. Zhang, and J. Zhong, "Application of neural networks to predict the elevated temperature flow behavior of a low alloy steel," *Comput. Mater. Sci.*, vol. 43, no. 4, pp. 752–758, Oct. 2008, doi: 10.1016/j.commatsci.2008.01.039.

[5] Y. C. Lin, X. Fang, and Y. P. Wang, "Prediction of metadynamic softening in a multi-pass hot deformed low alloy steel using artificial neural network," *J. Mater. Sci.*, vol. 43, no. 16, pp. 5508–5515, 2008, doi: 10.1007/s10853-008-2832-6.

[6] N. Haghdadi, A. Zarei-Hanzaki, A. R. Khalesian, and H. R. Abedi, "Artificial neural network modeling to predict the hot deformation behavior of an A356 aluminum alloy," *Mater. Des.*, vol. 49, pp. 386–391, Aug. 2013, doi: 10.1016/j.matdes.2012.12.082.

[7] U. Ali, W. Muhammad, A. Brahme, O. Skiba, and K. Inal, "Application of artificial neural networks in micromechanics for polycrystalline metals," *Int. J. Plast.*, 2019, doi: 10.1016/j.ijplas.2019.05.001.

[8] M. E. Haque and K. V. Sudhakar, "Prediction of corrosion-fatigue behavior of DP steel through artificial neural network," *Int. J. Fatigue*, 2001, doi: 10.1016/S0142-1123(00)00074-8.

[9] W. Zhang, Z. Bao, S. Jiang, and J. He, "An artificial neural network-based algorithm for evaluation of fatigue crack propagation considering nonlinear damage accumulation," *Materials (Basel).*, 2016, doi: 10.3390/ma9060483.

[10] P. Artymiak, L. Bukowski, J. Feliks, S. Narberhaus, and H. Zenner, "Determination of S-N curves with the application of artificial neural networks," *Fatigue Fract. Eng. Mater. Struct.*, 1999, doi: 10.1046/j.1460-2695.1999.00198.x.

[11] V. Venkatesh and H. J. Rack, "Neural network approach to elevated temperature creep-fatigue life prediction," *Int. J. Fatigue*, 1999, doi: 10.1016/S0142-1123(98)00071-1.

[12] W. Muhammad, A. P. Brahme, O. Ibragimova, J. Kang, and K. Inal, "A machine learning framework to predict local strain distribution and the evolution of plastic anisotropy & fracture in additively manufactured alloys," *Int. J. Plast.*, 2021, doi: 10.1016/j.ijplas.2020.102867.

[13] A. Derogar and F. Djavanroodi, "Artificial Neural Network

Modeling of Forming Limit Diagram," *Mater. Manuf. Process.*, vol. 26, no. 11, pp. 1415–1422, 2011, doi: 10.1080/10426914.2010.544818.

[14] N. S. Reddy, A. K. P. Rao, M. Chakraborty, and B. S. Murty, "Prediction of grain size of Al–7Si Alloy by neural networks," *Mater. Sci. Eng. A*, vol. 391, no. 1–2, pp. 131–140, Jan. 2005, doi: 10.1016/j.msea.2004.08.042.

[15] A. Brahme, M. Winning, and D. Raabe, "Prediction of cold rolling texture of steels using an Artificial Neural Network," *Comput. Mater. Sci.*, vol. 46, no. 4, pp. 800–804, 2009, doi: 10.1016/j.commatsci.2009.04.014.

[16] H. Çetinel, H. A. Özyiğit, and L. Özsoyeller, "Artificial neural networks modeling of mechanical property and microstructure evolution in the Tempcore process," *Comput. {&} Struct.*, vol. 80, no. 3–4, pp. 213–218, Feb. 2002, doi: 10.1016/S0045-7949(02)00016-0.

[17] R. Liu, A. Kumar, Z. Chen, A. Agrawal, V. Sundararaghavan, and A. Choudhary, "A predictive machine learning approach for microstructure optimization and materials design," *Sci. Rep.*, vol. 5, no. 1, p. 11551, 2015, doi: 10.1038/srep11551.

[18] K. Inal, P. D. Wu, and K. W. Neale, "Large strain behaviour of aluminium sheets subjected to in-plane simple shear," *Model. Simul. Mater. Sci. Eng.*, vol. 10, no. 2, pp. 237–252, 2002.

[19] W. Muhammad, A. Brahme, J. Kang, R. K. Mishra, and K. Inal, "Experimental and numerical investigation of texture evolution and the effects of intragranular backstresses in aluminum alloys subjected to large strain cyclic deformation," *Int. J. Plast.*, vol. 137, pp. 137–163, 2017.

[20] J. Kang *et al.*, "Constitutive Behavior of AA5754 Sheet Materials at Large Strains," *J. Eng. Mater. Technol.*, vol. 130, no. 3, p. 031004, 2008, doi: 10.1115/1.2931151.

[21] W. Muhammad, A. Brahme, J. Kang, R. Mishra, and K. Inal, "Large Strain Cyclic Simple Shear Behavior of Aluminum Extrusions: An Experimental and Numerical Study," in *Light Metals 2016*, 2016.

[22] W. Muhammad, M. Mohammadi, J. Kang, R. K. Mishra, and K. Inal, "An elasto-plastic constitutive model for evolving asymmetric/anisotropic hardening behavior of AZ31B and ZEK100 magnesium alloy sheets considering monotonic and reverse loading paths," *Int. J. Plast.*, vol. 70, pp. 30–59, 2015.

[23] D. Ghaffari Tari, M. J. J. Worswick, U. Ali, and M. A. A. Gharghouri, "Mechanical response of AZ31B magnesium alloy: Experimental characterization and material modeling considering proportional loading at room temperature," *Int. J. Plast.*, vol. 55, pp. 247–267, 2014, doi: 10.1016/j.ijplas.2013.10.006.

[24] W. Muhammad *et al.*, "Bendability enhancement of an age-hardenable aluminum alloy: Part II — multiscale numerical modeling of shear banding and fracture," *Mater. Sci. Eng. A*, 2019, doi: 10.1016/j.msea.2019.03.050.

[25] W. Muhammad, U. Ali, A. P. Brahme, J. Kang, R. K. Mishra, and K. Inal, "Experimental analyses and numerical modeling of texture evolution and the development of surface roughness during bending of an extruded aluminum alloy using a multiscale modeling framework," *Int. J. Plast.*, 2017, doi: 10.1016/j.ijplas.2017.09.013.

[26] J. Rossiter, A. Brahme, M. H. H. Simha, K. Inal, and R. K. Mishra, "A new crystal plasticity scheme for explicit time integration codes to simulate deformation in 3D microstructures: Effects of strain path, strain rate and thermal softening on localized deformation in the aluminum alloy 5754 during simple shear," *Int. J. Plast.*, vol. 26, no. 12, pp. 1702–1725, Dec. 2010, doi: 10.1016/j.ijplas.2010.02.007.

[27] R. J. Asaro and A. Needleman, "Texture Development and Strain Hardening In Rate Dependent Polyrystals," *Acta Metall.*, vol. 33, no. 42, pp. 923–953, 1985.

[28] Y. W. Chang and R. J. Asaro, "An Experimental Study of Shear Localization in Aluminum-Copper Single Crystals," *Acta Mater.*, vol. 29, pp. 241–257, 1981, doi: 10.1016/0001-6160(81)90103-6.

[29] P. D. Wu, K. W. Neale, and E. Van der Giessen, "On crystal plasticity FLD analysis," *Proceeding R. Soc. London*, vol. 453, pp. 1831–1848, 1997.

[30] D. F. Specht, "A general regression neural network," *Neural Networks, IEEE Trans.*, vol. 2, no. 6, pp. 568–576, 1991, doi: 10.1109/72.97934.

[31] C. M. Bishop, *Pattern Recognition And Machine Learning*. Springer, 2006.

[32] D. E. Rumelhart, G. E. Hinton, R. J. Williams, and others, "Learning representations by back-propagating errors," *Cogn. Model.*, vol. 5, no. 3, p. 1, 1988.

[33] M. Nielsen, "Neural Networks and Deep Learning," *Determ. Press*, 2015.

[34] Y. A. LeCun, L. Bottou, G. B. Orr, and K.-R. Müller, "Efficient BackProp," in *Neural Networks: Tricks of the Trade: Second Edition*, G. Montavon, G. B. Orr, and K.-R. Müller, Eds. Berlin, Heidelberg: Springer Berlin Heidelberg, 2012, pp. 9–48.

[35] G. Montavon and K.-R. Müller, "Deep Boltzmann machines and the centering trick," in *Neural Networks: Tricks of the Trade*, Springer, 2012, pp. 621–637.

[36] J. H. Holland, *Adaptation in Natural and Artificial Systems*. 2019.

[37] D. E. Goldberg, *Genetic algorithms in search, optimization, and machine learning*. 1989.